On heterogeneous coupling of multiscale methods for problems with and without scale separation

Assyr Abdulle[*] Orane Jecker[†]

Abstract

In this paper we discuss partial differential equations with multiple scales for which scale resolution are needed in some subregions, while a separation of scale and numerical homogenization is possible in the remaining part of the computational domain. Departing from the classical coupling approach that often relies on artificial boundary conditions computed from some coarse grain simulation, we propose a coupling procedure in which virtual boundary conditions are obtained from the minimization of a coarse grain and a fine scale model in overlapping regions where both models are valid. We discuss this method with a focus on interface control and a numerical strategy based on non-matching meshes in the overlap. A fully discrete a priori error analysis of the heterogeneous coupled multiscale method is derived and numerical experiments that illustrate the efficiency and flexibility of the proposed strategy are presented.

Key words. optimization, coupling, multiscale problems, virtual control, numerical homogenization

AMS subject classifications. 65N30, 35J15, 35B27,49J20

1 Introduction

The past few years has witnessed a growing number of new numerical schemes for multiscale problems. Broadly speaking, the numerical challenge for the approximation of such problems is to avoid scale resolution, i.e., the use of a fine mesh that resolves the smallest scale in the problem. Indeed such direct approaches are often computationally too expensive for practical applications. In this paper, we consider in a polygonal domain $\Omega \subset \mathbb{R}^d, d = 1, 2, 3$, with boundary $\Gamma = \Gamma_D \cup \Gamma_N$, the model problem

$$\begin{aligned} -\mathrm{div}\,(a^\varepsilon \nabla u^\varepsilon) &= f, \quad \text{in } \Omega, \\ u^\varepsilon &= g_D, \text{ on } \Gamma_D, \\ n \cdot (a^\varepsilon \nabla u^\varepsilon) &= g_N, \text{ on } \Gamma_N, \end{aligned} \tag{1}$$

where $f \in L^2(\Omega)$, $g_D \in H^{1/2}(\Gamma_D)$, and $g_N \in L^2(\Gamma_N)$, and where $a^\varepsilon \in (L^\infty(\Omega))^{d\times d}$ is a highly oscillatory tensor that satisfies, for $0 < \alpha < \beta$,

$$\alpha|\xi|^2 \le a^\varepsilon(x)\xi \cdot \xi, \quad |a^\varepsilon(x)\xi| \le \beta|\xi|, \quad \forall \xi \in \mathbb{R}^d, \text{ for a.e. } x \in \mathbb{R}. \tag{2}$$

[*]École Polytechnique Fédérale de Lausanne (assyr.abdulle@epfl.ch)
[†]École Polytechnique Fédérale de Lausanne (orane.jecker@epfl.ch)

For such a problem, one can identify two broad classes of multiscale methods, namely numerical methods that seek to approximate an effective solution of the original problems in which the small scales have been averaged out. The existence of such effective solutions usually relies on homogenization theory [9, 21]. The attractivity of such methods is the possibility to obtain numerical approximations that correctly describe the macroscopic behavior of the multiscale problem at a cost that however is independent of the smallest scale. Another class of multiscale methods aims at building coarse basis functions that encode the multiscale oscillations in the problem. This class of methods usually comes with a cost that is no longer independent of the small scale, but the construction of the basis functions can be localized and, once constructed, this basis can often be reused in a multi-query context. We refer to [5] for a review and references of the first class of methods and to [15, 20, 23] for review and references of the second class of methods. The framework that makes the first class of methods efficient is that of a simultaneous coupling of a macro and a micro method. In such approach a separation of the scales is often required. The second class of methods solves the fine scale problems on overlapping patches and it has recently been shown that convergences can also be obtained without assuming scale separation [20, 23].

In this contribution we address an intermediate situation between separated and non-separated scales in the following sense: we assume that in a subset ω_2 of the computational domain Ω the macro-micro upscaling strategy can be applied but that in an other part ω of the domain one needs full resolution of the scales. Here we assume that this second domain is sufficiently small so that standard resolved finite element method (FEM) can be used. While our method easily generalizes to multiple regions with and without scale separation, we assume here for simplicity that $\Omega = \omega_2 \cup \omega$. The main issue for such a coupling strategy is to set adequate boundary conditions at the interfaces of both computational domains. We note that such problems have numerous applications in the sciences, we mention for example heterogeneous structures with defects [16, 10] or steady flow problems with singularities [17]. Coupling strategies between fine scale and upscaled models have already been studied in the literature for example in [27] where a precomputed global homogenized solution is used to provide the boundary conditions in the fine scale subregions. More recently, a coupling strategy based on an L^2 projection of the homogenized solution onto harmonic fine scale functions has been discussed [8].

The aim of this paper is to pursue the study of a new approach that we have proposed in [6, 7] relying on an optimization based coupling strategy. By introducing small overlapping region ω_0 between ω_2 and ω, where both fine scale and homogenized model are valid, we consider the unknown boundary conditions for both models as (virtual) control and minimize the discrepancy of the solutions from the two models in the overlap. Two possible scenarios are illustrated in Figure 1. Such ideas have appeared earlier in the literature for coupling different type of partial differential equations [18] or for atomistic-to-continuum methods [28]. We also note, related to our method, the recent work on the coupling of local and nonlocal diffusion models [13].

We briefly describe the main contribution of this paper. First, in [7], the theory and the numerics have been developed for the cost function $\|\cdot\|_{\mathrm{L}^2(\omega_0)}$, called distributed observation in the classical terminology of optimal control. Here we consider the cost function $\|\cdot\|_{\mathrm{L}^2(\Gamma_1\cup\Gamma_2)}$, called boundary or interface control. Such controls can reduce the cost of the iterative method to solve the optimality system compared to the cost of solving the optimization problem with distributed control [14]. Second, in [7] we used the same mesh in the overlap ω_0 with the consequence of having to use a mesh size that scales with the fine mesh of ω. Here we discuss the use of independent meshes in the overlap through appropriate interpolation techniques. As a result, we have again a significant reduction in

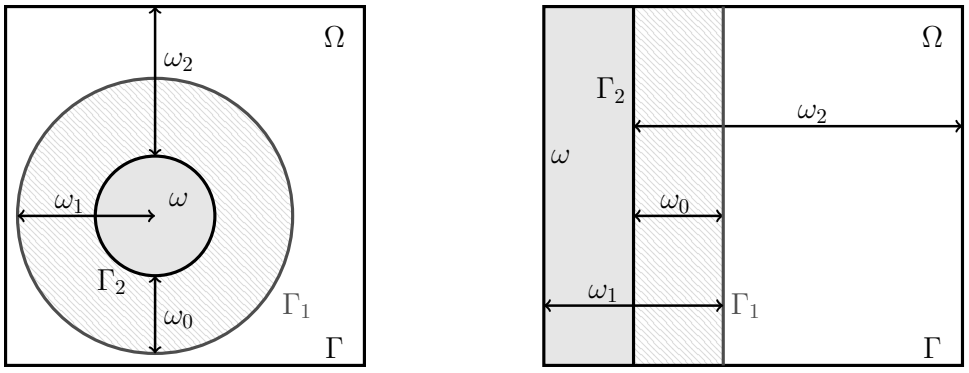

Figure 1: Two scenarios for the domain decomposition of Ω.

the computational cost of the coupling as the macroscopic numerical method in $\omega_2 = \Omega \setminus \omega$ does not need an increasing number of micro solvers as the mesh in ω_1 is refined. Finally, numerical examples were carried out in [7] only for the situation where $\omega \Subset \Omega$ (Figure 1 left), here we discuss also the scenario for which $\partial\omega \cap \partial\Omega \neq \emptyset$ (Figure 1 right).

The paper is organized as follows. In Section 2, we describe the model problem, introduce the two minimization costs functions considered in this paper, and give an a priori error analysis between the coupled and the fine scale solutions. In Section 3 we define the multiscale numerical discretization of the optimization problem and perform a fully discrete a priori error analysis. Finally Section 4 contains several numerical experiments that illustrate the theoretical results and the performance of the new coupling strategy.

Notations. In what follows, $C > 0$ is used to denote a generic constant independent of ε. We consider the usual Sobolev space $H^1(\Omega) = \{u \in L^2(\Omega) \mid D^r u \in L^2(\Omega), |r| \leq 1\}$, where $r \in \mathbb{N}^d, |r| = r_1 + \ldots + r_d$ and $D^r = \partial_1^{r_1} \ldots \partial_d^{r_d}$. The notation $|\cdot|$ stands for the standard Euclidean norm in $\mathbb{R}^d$. Let Y denote the unit cube $(0,1)^d$ and define $W^1_{\text{per}}(Y) := \{v \in H^1_{\text{per}}(Y) \mid \int_Y v \mathrm{d}y = 0\}$ where the set $H^1_{\text{per}}(Y)$ is the closure of $\mathcal{C}^\infty_{\text{per}}(Y)$ for the H^1 norm.

2 Problem formulation

Let $\omega \subset \Omega$ be the region without scale separation and ω_0 be the overlap region. Assume that $\Gamma_1 = \partial\omega_1 \setminus \Gamma$ and $\Gamma_2 = \partial\omega_2 \setminus \Gamma$ are Lipschitz continuous boundaries. We decompose the tensor a^ε of problem (1) into $a^\varepsilon = a_\omega + a_2^\varepsilon$, where $a_2^\varepsilon = a^\varepsilon \mathbb{1}_{\omega_2}$ and $a_\omega = a^\varepsilon \mathbb{1}_\omega$ are tensors with and without scale separation, respectively. The tensor a_2^ε H-converges towards an homogenized tensor a_2^0 [25]. Further, we set $a_1 = a^\varepsilon \mathbb{1}_{\omega_1}$, $u_1 = u_1^\varepsilon$, and $u_2 = u_2^0$. The heterogeneous control restricted to Dirichlet boundary controls is given by the following problem: find $u_1^\varepsilon \in H^1(\omega_1)$ and $u_2^0 \in H^1(\omega_2)$, such that $\frac{1}{2}\|u_1^\varepsilon - u_2^0\|^2_{\mathcal{H}}$ is minimized under the following constraints, for $i = 1, 2$,

$$\begin{aligned} -\text{div}\,(a_i \nabla u_i) &= f, && \text{in } \omega_i, \\ u_i &= \theta_i, && \text{on } \Gamma_i, \\ u_i &= g_D, && \text{on } \partial\omega_i \cap \Gamma_D, \\ n \cdot (a_i \nabla v_i) &= g_N, && \text{on } \partial\omega_i \cap \Gamma_N, \end{aligned} \tag{3}$$

where the boundary conditions θ_i, called the virtual controls, are to be determined; $(\mathcal{H}, \|\cdot\|_{\mathcal{H}})$ is a Hilbert space specified below. Further we define the space of admissible Dirichlet controls

$$\mathcal{U}_i^D = \{\mu_i \in H^{1/2}(\Gamma_i) \mid \exists u \in H^1(\omega_i), u|_{\Gamma_i} = \mu_i, \text{ in the sense of the trace}\}.$$

The strategy is to solve a minimization problem in the space of admissible controls, where we minimize the cost

$$J(\theta_1, \theta_2) = \frac{1}{2}\|u_1^\varepsilon(\theta_1) - u_2^0(\theta_2)\|_{\mathcal{H}}^2.$$

In this paper, two Hilbert spaces $(\mathcal{H}, \|\cdot\|_{\mathcal{H}})$ are considered.
Case 1. Minimization in $L^2(\omega_0)$, with

$$J(\theta_1, \theta_2) = \frac{1}{2}\|u_1^\varepsilon(\theta_1) - u_2^0(\theta_2)\|_{\mathrm{L}^2(\omega_0)}^2. \tag{case 1}$$

Case 2. Minimization in $L^2(\Gamma_1 \cup \Gamma_2)$, with

$$J(\theta_1, \theta_2) = \frac{1}{2}\|u_1^\varepsilon(\theta_1) - u_2^0(\theta_2)\|_{\mathrm{L}^2(\Gamma_1\cup\Gamma_2)}^2. \tag{case 2}$$

The solutions are split into

$$u_1^\varepsilon(\theta_1) = u_{1,0}^\varepsilon + v_1^\varepsilon(\theta_1), \quad u_2^0(\theta_2) = u_{2,0}^0 + v_2^0(\theta_2),$$

where (v_1^ε, v_2^0) are called the state variables and satisfy, for $i = 1, 2$,

$$\begin{cases} -\mathrm{div}\,(a_i \nabla v_i) &= 0, \quad \text{in } \omega_i, \\ v_i &= \theta_i, \quad \text{on } \Gamma_i, \\ v_i &= 0, \quad \text{on } \partial\omega_i \cap \Gamma_D, \\ n \cdot (a_i \nabla v_i) &= 0, \quad \text{on } \partial\omega_i \cap \Gamma_N, \end{cases} \tag{4}$$

where $v_1 = v_1^\varepsilon$, and $v_2 = v_2^0$. The functions $u_{i,0}$ are solutions of problem (3) with zero controls on Γ_i, for $i = 1, 2$. Let $H_D^1(\omega_i)$, $i = 1, 2$, denote the functions in $H^1(\omega_i)$ that vanish on $\partial\omega_i \cap \Gamma_D$. The solutions $u_{1,0}^\varepsilon$ and $u_{2,0}^0$ exist and are unique, thank to the Lax-Milgram Lemma, and the solutions v_1^ε and v_2^0 can be uniquely determined if the controls θ_1 and θ_2 are known. As $u_{1,0}^\varepsilon$ and $u_{2,0}^0$ are independent of the virtual controls (θ_1, θ_2), they can be computed beforehand.
The well-posedness of the optimization problem is proved following Lions [22]. The key point consists in proving that the cost function induces a norm over $\mathcal{U} = (\mathcal{U}_1^D, \mathcal{U}_2^D)$. One consider then the completion of $\mathcal{U}$ (still denoted by $\mathcal{U}$) with respect to the cost induced norm, and the minimization problem admits a unique solution $(\theta_1, \theta_2) \in \mathcal{U}$ satisfying the Euler-Lagrange formulation

$$\int_{\mathcal{O}} (v_1^\varepsilon(\theta_1) - v_2^0(\theta_2))(v_1^\varepsilon(\mu_1) - v_2^0(\theta_2))\mathrm{d}x = -\int_{\mathcal{O}} (v_1^\varepsilon(\mu_1) - v_2^0(\mu_2))(u_{1,0}^\varepsilon - u_{2,0}^0)\mathrm{d}x, \tag{5}$$

for all $(\mu_1, \mu_2) \in \mathcal{U}$, and where $\mathcal{O}$ is either ω_0 or $\Gamma_1 \cup \Gamma_2$. While the optimization problem with the cost function of case 1 has been considered in [7], we prove that the optimal controls problem is well-posed with the cost function of case 2.
For the homogenization theory (H-convergence), we consider a family of problems (1) indexed by ε. In what follows, we will often assume $\varepsilon \leq \varepsilon_0$, where ε_0 is a parameter used in a strong Cauchy-Schwarz inequality (see Lemma 5.3). We assume that $\theta_i \in \mathcal{U}_i^D$ and hence $u_i(\theta_i)$ is in $H^1(\omega_i)$, for $i = 1, 2$.

2.1 Minimization over $\Gamma_1 \cup \Gamma_2$

As a fist step, we write the cost in terms of the state variables v_1^ε and v_2^0,

$$J(\theta_1,\theta_2) = \frac{1}{2}\|v_1^\varepsilon(\theta_1) - v_2^0(\theta_2)\|^2_{\mathrm{L}^2(\Gamma_1\cup\Gamma_2)} + \|(v_1^\varepsilon(\theta_1) - v_2^0(\theta_2))(u_{1,0}^\varepsilon - u_{2,0}^0)\|^2_{\mathrm{L}^2(\Gamma_1\cup\Gamma_2)} + \frac{1}{2}\|u_{1,0}^\varepsilon - u_{2,0}^0\|^2_{\mathrm{L}^2(\Gamma_1\cup\Gamma_2)}.$$

We set

$$\pi((\theta_1,\theta_2),(\mu_1,\mu_2)) = \int_{\Gamma_1\cup\Gamma_2}(v_1^\varepsilon(\theta_1) - v_2^0(\theta_2))(v_1^\varepsilon(\mu_1) - v_2^0(\theta_2))\mathrm{d}x$$

and show that π induce a norm over $\mathcal{U}$.

Lemma 2.1 *The bilinear form π is a scalar product over $\mathcal{U}$.*

Proof. The symmetry and positivity are clear, and it remains to prove that the form is positive definite; $\pi(\theta_1,\theta_2) = 0$ if and only if $\theta_1 = 0$ and $\theta_2 = 0$. We use the short-hand notation $\pi(\theta_1,\theta_2)$ to denote $\pi((\theta_1,\theta_2),(\theta_1,\theta_2))$.
Assuming that θ_1 and θ_2 are zero, the state variables v_1^ε and v_2^0 are solutions of boundary value problems with zero data, thus v_1^ε and v_2^0 are zero over ω_1 and ω_2 respectively. This leads to $\pi(\theta_1,\theta_2) = 0$.
Assume now that $\pi(\theta_1,\theta_2) = 0$. It holds that

$$\int_{\Gamma_1\cup\Gamma_2}(v_1^\varepsilon(\theta_1) - v_2^0(\theta_2))^2\mathrm{d}x = \int_{\Gamma_1}(\theta_1 - v_2^0(\theta_2))^2\mathrm{d}x + \int_{\Gamma_2}(v_1^\varepsilon(\theta_1) - \theta_2)^2\mathrm{d}x = 0,$$

and

$$\int_{\Gamma_1}(\theta_1 - v_2^0(\theta_2))^2\mathrm{d}x = 0, \qquad \int_{\Gamma_2}(v_1^\varepsilon(\theta_1) - \theta_2)^2\mathrm{d}x = 0. \tag{6}$$

This implies that $v_1^\varepsilon(\theta_1)|_{\Gamma_1} = \theta_1 = v_2^0(\theta_2)|_{\Gamma_1}$ a.e., and $v_2^0(\theta_2)|_{\Gamma_2} = \theta_2 = v_1^\varepsilon|_{\Gamma_2}(\theta_1)$ a.e. As v_1^ε and v_2^0 are H^1 functions on ω_1 and ω_2 respectively, we obtain

$$\|\theta_1 - v_2^0(\theta_2)\|_{\mathrm{H}^{1/2}(\Gamma_1)} = 0, \text{ and } \|v_1^\varepsilon(\theta_1) - \theta_2\|_{\mathrm{H}^{1/2}(\Gamma_2)} = 0.$$

Using the trace inequality and the strong Cauchy-Schwarz inequality Appendix 5.3, it holds

$$\begin{aligned} 0 = \|v_1^\varepsilon(\theta_1) - v_2^0(\theta_2)\|^2_{\mathrm{H}^{1/2}(\Gamma_1\cup\Gamma_2)} &\geq C_1\|v_1^\varepsilon(\theta_1) - v_2^0(\theta_2)\|^2_{\mathrm{H}^1(\omega_0)} \\ &\geq C_1\|v_1^\varepsilon(\theta_1) - v_2^0(\theta_2)\|^2_{\mathrm{L}^2(\omega_0)} \\ &\geq C_2(\|v_1^\varepsilon(\theta_1)\|^2_{\mathrm{L}^2(\omega_0)} + \|v_2^0(\theta_2)\|^2_{\mathrm{L}^2(\omega_0)}), \\ &\geq C_3(\|v_1^\varepsilon(\theta_1)\|^2_{\mathrm{L}^2(\omega_1)} + \|v_2^0(\theta_2)\|^2_{\mathrm{L}^2(\omega_2)}), \end{aligned}$$

where the last inequality comes from the Caccioppoli inequality Appendix 5.1, the inequality given in Appendix 5.2, and the PoincarÃ© inequality. We obtain that

$$v_1^\varepsilon \equiv 0 \text{ a.e. on } \omega_1, \text{ and } v_2^0 \equiv 0 \text{ a.e. on } \omega_2,$$

hence $\theta_1 = \theta_2 = 0$, thanks to (6). This concludes the proof. □

The norm induced from the scalar product π is given by

$$\|(\mu_1,\mu_2)\|_{\mathrm{L}^*(\mathcal{U})} := \left(\int_{\mathcal{O}} (v_1^\varepsilon(\mu_1) - v_2^0(\mu_2))^2 \mathrm{d}x\right)^{1/2}, \quad \forall (\mu_1,\mu_2) \in \mathcal{U}, \tag{7}$$

where $\mathcal{O}$ is either ω_0 or $\Gamma_1 \cup \Gamma_2$.

2.2 A priori error analysis

Let u^ε be the solution of the heterogeneous problem (1), and let us derive a priori error bounds between u^ε and the solution of the coupling

$$\bar{u} = \begin{cases} u_1^\varepsilon(\theta_1), & \text{in } \omega^+, \\ u_2^{rec}(\theta_2), & \text{in } \Omega \setminus \omega^+, \end{cases} \tag{8}$$

where u_2^{rec} is the reconstructed homogeneous solution u_2^0 with periodic correctors, and ω^+ is a subdomain of Ω such that $\omega \subseteq \omega^+ \subseteq \omega_1$. The term u_2^{rec} is given by

$$u_2^{rec}(x) = u_2^0(x) + \varepsilon \sum_{j=1}^{d} \chi^j(x, x/\varepsilon) \frac{\partial u_2^0(x)}{\partial x_j}, \quad x \in \Omega \setminus \omega^+, \tag{9}$$

where $u_2^0 = u_2^0(\theta_2)$.
We consider the cost function of case 2, and we refer to [7] for an analysis of case 1. For ε fixed, we define u^0 as the solution of

$$\begin{array}{rll} -\mathrm{div}\,(a_2^0 \nabla u^0) &= f, & \text{in } \omega_2, \\ u^0 &= \gamma_2(u^\varepsilon), & \text{on } \Gamma_2, \\ u^0 &= g_D, & \text{on } \partial\omega_2 \cap \Gamma_D, \\ n \cdot (a_2^0 \nabla u^0) &= g_N, & \text{on } \partial\omega_2 \cap \Gamma_N, \end{array} \tag{10}$$

where $\gamma_2 : H^1(\omega_2) \to H^{1/2}(\Gamma_2)$ denotes the trace operator on Γ_2. Similarly, we define the trace operator γ_1 on Γ_1. Assuming that the tensor a_2^ε is periodic in the fast variable, i.e., $a_2^\varepsilon(x) = a_2(x, x/\varepsilon) = a_2(x,y)$ is Y-periodic in y, where $Y = (0,1)^d$, explicit equations are available to compute the homogenized tensor a_2^0

$$a_2^0(x) = \frac{1}{|Y|} \int_Y a_2(x,y)\,(I + \nabla\chi)\,\mathrm{d}y,$$

where $\nabla\chi = (\nabla\chi^1, \ldots, \nabla\chi^d)$ and I is the $d \times d$ identity matrix. The functions $\chi^j \in W^1_{per}(Y)$ are called the first order correctors and, for $j = 1, \ldots, d$, χ^j is solution of the cell problem

$$\int_Y a_2(x,y) \nabla\chi^j \cdot \nabla v \mathrm{d}y = -\int_Y a_2(x,y) e_j \nabla v \mathrm{d}y, \quad \forall v \in W^1_{per}(Y),$$

with periodic boundary conditions, and where $(e_i)_{i=1}^d$ denotes the canonical basis of $\mathbb{R}^d$. Assuming sufficient regularity on u^0 and on χ^j, it can be proved that

$$\|u^\varepsilon - u^0\|_{\mathrm{L}^2(\omega_2)} \leq C\varepsilon, \tag{11}$$

where the constant is independent of ε. For proofs, we refer to [9, 21, 24].

Estimates for the fine solution Let us define an operator $P : \mathcal{U} \to H^1(\omega_1) \times H^1(\Omega \setminus \omega_1)$ such that

$$P(\mu_1, \mu_2) \mapsto \begin{cases} u_1^\varepsilon(\mu_1), \text{ in } \omega_1, \\ u_2^0(\mu_2), \text{ in } \Omega \setminus \omega_1. \end{cases}$$

It can be split into $P = Q + U_0$, where $Q : \mathcal{U} \to H^1(\omega_1) \times H^1(\Omega \setminus \omega_1)$ is defined by

$$Q(\mu_1, \mu_2) \mapsto \begin{cases} v_1^\varepsilon(\mu_1), \text{ in } \omega_1, \\ v_2^0(\mu_2), \text{ in } \Omega \setminus \omega_1, \end{cases}$$

where the state variables v_1^ε and v_2^0 are solutions of (4) for $i = 1, 2$ respectively, and where U_0 is given by

$$U_0 = \begin{cases} u_{1,0}^\varepsilon, \text{ in } \omega_1, \\ u_{2,0}^0, \text{ in } \Omega \setminus \omega_1. \end{cases}$$

For the cost function of case 1, it has been shown in [7] that the operator Q is bounded in the operator norm, i.e.,

$$\|Q\| := \sup_{(\mu_1,\mu_2)\in\mathcal{U}} \frac{Q(\mu_1, \mu_2)}{\|(\mu_1, \mu_2)\|_{\mathrm{L}^*(\mathcal{U})}} \leq C.$$

Here we assume that Q is bounded for the norm in $\mathcal{U}$ induced by the scalar product (7) for the cost function of case 2.

Theorem 2.2 *Let u^ε be solution of (1) and $\bar{u}$ be given by (8). Assume that u^0 and χ^j are smooth enough for (11) to hold, and that $\|Q\| \leq C$. Then we have*

$$\|u^\varepsilon - \bar{u}\|_{\mathrm{H}^1(\omega^+)} \leq C\varepsilon,$$

where the constant C depends on the constant of the Caccioppoli inequality, the bound $\|Q\|$, and the trace constants associated to the trace operators γ_1 and γ_2 on Γ_1 and Γ_2, respectively.

The difference $u^\varepsilon - \bar{u}$ is a_1^ε-harmonic in ω_1, thus Caccioppoli inequality (see Appendix 5.1) can be applied,

$$\begin{aligned} \|u^\varepsilon - \bar{u}\|_{\mathrm{H}^1(\omega^+)} &\leq C\frac{1}{\tau}\|u^\varepsilon - \bar{u}\|_{\mathrm{L}^2(\omega_1)} \\ &= C\frac{1}{\tau}\|P(\gamma_1(u^\varepsilon), \gamma_2(u^\varepsilon)) - P(\theta_1, \theta_2)\|_{\mathrm{L}^2(\omega_1)} \\ &\leq \frac{C}{\tau}\|Q\|\|(\gamma_1(u^\varepsilon), \gamma_2(u^\varepsilon)) - (\theta_1, \theta_2)\|_{\mathrm{L}^*(\mathcal{U})}. \end{aligned} \tag{12}$$

We next need to bound $\|(\gamma_1(u^\varepsilon), \gamma_2(u^\varepsilon)) - (\theta_1, \theta_2)\|_{\mathrm{L}^*(\mathcal{U})}$.

Lemma 2.3 *Let u^ε and u^0 solve (1) and (10) respectively, and let $(\theta_1, \theta_2) \in \mathcal{U}$ be the optimal virtual controls. Then*

$$\|(\gamma_1(u^\varepsilon), \gamma_2(u^\varepsilon)) - (\theta_1, \theta_2)\|_{\mathrm{L}^*(\mathcal{U})} \leq \|u^\varepsilon - u^0\|_{\mathrm{L}^2(\Gamma_1\cup\Gamma_2)}.$$

Proof. From the definition, it holds

$$\|(\gamma_1(u^\varepsilon),\gamma_2(u^\varepsilon))-(\theta_1,\theta_2)\|_{\mathrm{L}^*(\mathcal{U})}=\sup_{(\mu_1,\mu_2)\in\mathcal{U}}\frac{|\pi((\gamma_1(u^\varepsilon),\gamma_2(u^\varepsilon)),(\mu_1,\mu_2))-\pi((\theta_1,\theta_2),(\mu_1,\mu_2))|}{\|(\mu_1,\mu_2)\|_{\mathrm{L}^*(\mathcal{U})}}.$$

We look at the numerator. As the pair (θ_1,θ_2) minimizes the cost function J, the Euler-Lagrange formulation (5) holds and

$$\begin{aligned}
&\pi((\gamma_1(u^\varepsilon),\gamma_2(u^\varepsilon)),(\mu_1,\mu_2))-\pi((\theta_1,\theta_2),(\mu_1,\mu_2))=\\
&=\int_{\Gamma_1\cup\Gamma_2}(v_1^\varepsilon(\gamma_1(u^\varepsilon))-v_2^0(\gamma_2(u^\varepsilon)))(v_1^\varepsilon(\mu_1)-v_2^0(\mu_2))\mathrm{d}x\\
&\quad+\int_{\Gamma_1\cup\Gamma_2}(v_1^\varepsilon(\mu_1)-v_2^0(\mu_2))(u_{1,0}^\varepsilon-u_{2,0}^0)\mathrm{d}x\\
&=\int_{\Gamma_1\cup\Gamma_2}((v_1^\varepsilon(\gamma_1(u^\varepsilon))+u_{1,0}^\varepsilon)-(v_2^0(\gamma_2(u^\varepsilon))+u_{2,0}^0))(v_1^\varepsilon(\mu_1)-v_2^0(\mu_2))\mathrm{d}x\\
&=\int_{\Gamma_1\cup\Gamma_2}(u^\varepsilon-u^0)(v_1^\varepsilon(\mu_1)-v_2^0(\mu_2))\mathrm{d}x\le\|u^\varepsilon-u^0\|_{\mathrm{L}^2(\Gamma_1\cup\Gamma_2)}\|(\mu_1,\mu_2)\|_{\mathrm{L}^*(\mathcal{U})}.
\end{aligned}$$

The result follows. □

The next Lemma gives an upper bound to the norm in Lemma 2.3.

Lemma 2.4 *Let u^ε and u^0 be solution of* (1) *and* (10) *respectively. Assume that u^0 and χ^j have enough regularity for* (11) *to hold. Then*

$$\|u^\varepsilon-u^0\|_{\mathrm{L}^2(\Gamma_1\cup\Gamma_2)}\le C\varepsilon,$$

where the constant C is independent of ε.

Proof. It holds

$$\|u^\varepsilon-u^0\|_{\mathrm{L}^2(\Gamma_1\cup\Gamma_2)}\le\|u^\varepsilon-u^0\|_{\mathrm{L}^2(\Gamma_1)}+\|u^\varepsilon-u^0\|_{\mathrm{L}^2(\Gamma_2)}.$$

Using the continuity of the traces, the first term can be bounded by

$$\|u^\varepsilon-u^0\|_{\mathrm{L}^2(\Gamma_1)}\le C\|u^\varepsilon-u^0\|_{\mathrm{L}^2(\omega_2)}\le C\varepsilon,$$

whereas the second term is zero because $u^0|_{\Gamma_2}=\gamma_2(u^\varepsilon)=u^\varepsilon|_{\Gamma_2}$. This prove the result. □

The proof of Theorem 2.2 follows from (12) and Lemmas 2.3 and 2.4.

Estimates for the coarse solution The a priori error estimates to the coarse scale solver follows from [7, Theorem 3.6] using Lemma 2.4. We skip the details.

Theorem 2.5 *Let u^ε be solution of* (1) *and $u_2^{rec}(\theta_2)$ be given by* (9). *Let $a_2(x,y)\in\mathcal{C}(\overline{\omega}_2;L^\infty_{per}(Y))$ and $\chi^j\in W_{per}(Y)$, $j=1,\dots,d$. If in addition, $u^\varepsilon\in H^2(\Omega)$, $u_2^0(\theta_2)\in H^2(\omega_2)$, and $\chi^j\in W^{1,\infty}(Y)$, $j=1,\dots,d$, it holds*

$$\|u^\varepsilon-u_2^{rec}(\theta_2)\|_{\mathrm{H}^1(\Omega\setminus\omega^+)}\le C\varepsilon^{1/2},$$

where the constant C is independent of ε, but depends on τ, τ^+, and the ellipticity constants of a_2^ε.

3 Fully discrete coupling method

In this section, we describe the fully discrete overlapping coupling method, and perform an a priori error analysis. The fine scale solver requires a triangulation of size $\tilde{h}$ sufficiently small to resolve the multiscale nature of the tensor. In contrast, the coarse scale solver on ω_2 takes full advantage of the scale separation and allows for a mesh size larger than the fine scale. We use the FEM in ω_1 and the FE-HMM in ω_2. As the finite elements of the fine and coarse meshes in ω_0 are different, an interpolation between the two meshes should be considered. One can also chose to use the same finite elements in the overlap, leading to a discontinuity at Γ_1 in the mesh over ω_2. In that latter situation, the discontinuous Galerkin FE-HMM [4] should be used instead of the FE-HMM.
In what follows, we consider for simplicity the problem (1) with homogeneous Dirichlet boundary conditions, i.e., we set $g_D = 0$ and $\Gamma_N = \emptyset$. Further, we assume that the strong Cauchy-Schwarz Lemma (Appendix 5.3) and its discrete version (Appendix 5.5) hold.

Numerical method for the fine scale problem. Let $\mathcal{T}_{\tilde{h}}$ be a partition of ω_1, in simplicial or quadrilateral elements, with mesh size $\tilde{h} \ll \varepsilon$ where $\tilde{h} = \max_{K\in\mathcal{T}_{\tilde{h}}} h_K$, and h_K is the diameter of the element K. In addition, we suppose that the family of partitions $\{\mathcal{T}_{\tilde{h}}\}$ is admissible and shape regular [11], i.e.,

(T1) **admissible:** $\overline{\omega}_1 = \cup_{K\in\mathcal{T}_h} K$ and the intersection of two elements is either empty, a vertex, or a common face;

(T2) **shape regular:** there exists $\sigma > 0$ such that $h_K/\rho_K \leq \sigma$, for all $K \in \mathcal{T}_{\tilde{h}}$ and for all $\mathcal{T}_{\tilde{h}} \in \{\mathcal{T}_{\tilde{h}}\}$, where ρ_K is the diameter of the largest circle contained in the element K.

For each partition $\mathcal{T}_{\tilde{h}}$ of the family $\{\mathcal{T}_{\tilde{h}}\}$, we define a FE space in ω_1

$$V_D^p(\omega_1, \mathcal{T}_{\tilde{h}}) = \{w \in H_D^1(\omega_1) \mid w_{|_K} \in \mathcal{R}^p(K),\ \ \forall K \in \mathcal{T}_{\tilde{h}}\},$$

where $\mathcal{R}^p$ is the space $\mathcal{P}^p$ of polynomials of degree at most p on K if K is a triangle, and the space $\mathcal{Q}^p$ of polynomials of degree at most p in each variable if K is a rectangle. Further, $V_0^p(\omega_1, \mathcal{T}_{\tilde{h}})$ denotes the space of functions in $V_D^p(\omega_1, \mathcal{T}_{\tilde{h}})$ that vanish on $\partial\omega_1$.
Let $u_{1,\tilde{h}}$ be the numerical approximation of u_1^ε satisfying problem (3) for $i = 1$. We can split $u_{1,\tilde{h}}$ into $u_{1,\tilde{h}} = u_{1,0,\tilde{h}} + v_{1,\tilde{h}}$, where $v_{1,\tilde{h}} \in V_D^p(\omega_1, \mathcal{T}_{\tilde{h}})$ is obtained by the optimization method and $u_{1,0,\tilde{h}} \in V_0^p(\omega_1, \mathcal{T}_{\tilde{h}})$ satisfies

$$B_1(u_{1,0,\tilde{h}}, w_{1,\tilde{h}}) = \int_{\omega_1} a_1 \nabla u_{1,0,\tilde{h}} \cdot \nabla w_{1,\tilde{h}} \mathrm{d}x = F_1(w_{1,\tilde{h}}), \quad \forall w_{1,\tilde{h}} \in V_0^p(\omega_1, \mathcal{T}_{\tilde{h}}),$$

where F_1 is given by

$$F_1(w_{1,\tilde{h}}) = \int_{\omega_1} f w_{1,\tilde{h}} \mathrm{d}x.$$

Thanks to the Poincaré inequality, the coercivity and boundedness of the bilinear form B_1 can be proved; the existence and uniqueness of $u_{1,0,\tilde{h}}$ follows.

Numerical method for the coarse scale problem. Let $\{\mathcal{T}_H\}$ be a family of admissible (T1) and shape regular (T2) partitions of ω_2, with mesh size $H = \max_{K\in\mathcal{T}_H} h_K$. For each partition $\mathcal{T}_H$ of the family $\{\mathcal{T}_H\}$, we define a FE space over ω_2

$$V_D^p(\omega_2, \mathcal{T}_H) = \{v \in H_D^1(\omega_2) \mid w_{|_K} \in \mathcal{R}^p(K), \ \ \forall K \in \mathcal{T}_H\},$$

and use $V_0^p(\omega_2, \mathcal{T}_H)$ to denote the set of functions of $V_D^p(\omega_2, \mathcal{T}_H)$ that vanish over $\partial\omega_2$.

Quadrature formula. A macroscopic quadrature formula is given by the pair $\{x_{j,K}, \omega_{j,K}\}$ of quadrature nodes $x_{j,K}$ and weights $\omega_{j,K}$, for $j = 1, \ldots, J$. The sampling domain of size δ around each quadrature point is denoted by $K_{\delta_j} = x_{j,K} + \delta[-1/2, 1/2]^d$. We assume that the quadrature formula verifies the necessary assumptions to guarantee that the standard error estimates for a FEM hold [11].

The numerically homogenized tensor $a_2^{0,h}(x_{j,K})$ is obtained using numerical solutions of micro problems defined in K_{δ_j}. In each sampling domain, we consider a mesh $\mathcal{T}_h$ in simplicial or quadrilateral elements K with mesh size $h = \max_{K\in\mathcal{T}_h} h_K$ satisfying $h < \varepsilon$. The micro FE space is

$$S^q(K_{\delta_j}, \mathcal{T}_h) = \{w^h \in W(K_{\delta_j}) \mid w^h_{|_K} \in \mathcal{R}^q(K), \ \ \forall K \in \mathcal{T}_h\},$$

where the space $W(K_{\delta_j})$ depends on the boundary conditions in the micro problems; $W(K_{\delta_j}) = H_0^1(K_{\delta_j})$ for Dirichlet coupling, or $W(K_{\delta_j}) = W^1_{\text{per}}(K_{\delta_j})$ for periodic coupling. The discrete micro problems read: find $\psi^{i,h}_{K_{\delta_j}} \in S^q(K_{\delta_j}, \mathcal{T}_h)$, $i = 1, \ldots, d$, solution of

$$\int_{K_{\delta_j}} a_2^\varepsilon(x)\nabla\psi^{i,h}_{K_{\delta_j}} \cdot \nabla w_j^h \mathrm{d}x = -\int_{K_{\delta_j}} a_2^\varepsilon(x) e_i \nabla w_j^h \mathrm{d}x, \quad \forall w_j^h \in S^1(K_{\delta_j}, \mathcal{T}_h). \tag{13}$$

The numerically homogenized tensor can be computed by

$$a_2^{0,h}(x_{j,K}) = \frac{1}{|K_{\delta_j}|}\int_{K_{\delta_j}} a_2^\varepsilon(x)\left(I + \nabla\psi^h_{K_{\delta_j}}\right)\mathrm{d}x,$$

where $\nabla\psi^h_{K_{\delta_j}} = (\nabla\psi^{1,h}_{K_{\delta_j}}, \ldots, \nabla\psi^{d,h}_{K_{\delta_j}})$. We define a macro bilinear form $B_{2,H}(\cdot,\cdot)$ over $V_D^p(\omega_2, \mathcal{T}_H) \times V_D^p(\omega_2, \mathcal{T}_H)$,

$$B_{2,H}(v_{2,H}, w_{2,H}) \ = \sum_{K\in\mathcal{T}_H}\sum_{j=1}^{J} \omega_{j,K} a_2^{0,h}(x_{j,K})\nabla v_{2,H}(x_{j,K}) \cdot \nabla w_{2,H}(x_{j,K}).$$

The numerical homogenized solution $u_{2,H}$ is split into $u_{2,H} = u_{2,0,H} + v_{2,H}$, where $v_{2,H} \in V_D^p(\omega_2, \mathcal{T}_H)$ is given by the coupling and $u_{2,0,H} \in V_0^p(\omega_2, \mathcal{T}_H)$ is the solution of

$$B_{2,H}(u_{2,0,H}, w_{2,H}) = F_2(w_{2,H}), \quad \forall w_{2,H} \in V_0^p(\omega_2, \mathcal{T}_H),$$

with F_2 given by

$$F_2(w_{2,H}) = \int_{\omega_2} f w_{2,H} \mathrm{d}x.$$

Numerical Algorithm In this section, we state the discrete coupling and give the main convergence results. The well-posedness and the proofs of the errors estimates are done in details in [7]. In what follows, we use $\mathcal{O}$ to denote either ω_0 or $\Gamma_1 \cup \Gamma_2$.
The solution $(u_{1,\tilde{h}}, u_{2,H}) \in V_D^p(\omega_1, \mathcal{T}_{\tilde{h}}) \times V_D^p(\omega_2, \mathcal{T}_H)$ satisfies

$$\min_{\mu_{1,\tilde{h}}, \mu_{2,H}} \frac{1}{2} \|u_{1,\tilde{h}}(\mu_{1,\tilde{h}}) - u_{2,H}(\mu_{2,H})\|^2_{\mathrm{L}^2(\mathcal{O})} \text{ subject to } \begin{cases} B_1(u_{1,\tilde{h}}, w_{1,\tilde{h}}) & = F_1(w_{1,\tilde{h}}), \\ B_{2,H}(u_{2,H}, w_{2,H}) & = F_2(w_{2,H}), \end{cases}$$

for all $w_{1,\tilde{h}} \in V_0^p(\omega_1, \mathcal{T}_{\tilde{h}})$ and $w_{2,H} \in V_0^p(\omega_2, \mathcal{T}_H)$. We introduce discrete Lagrange multipliers for each of the constraints, and obtain a discrete optimality system: find $(v_{1,\tilde{h}}, \lambda_{1,\tilde{h}}, v_{2,H}, \lambda_{2,H}) \in V_D^p(\omega_1, \mathcal{T}_{\tilde{h}}) \times V_0^p(\omega_1, \mathcal{T}_{\tilde{h}}) \times V_D^p(\omega_2, \mathcal{T}_H) \times V_0^p(\omega_2, \mathcal{T}_H)$ satisfying

$$\int_{\mathcal{O}} (v_{1,\tilde{h}} - v_{2,H}) w_{1,\tilde{h}} \mathrm{d}x - B_1(w_{1,\tilde{h}}, \lambda_{1,\tilde{h}}) = -\int_{\mathcal{O}} (u_{1,0,\tilde{h}} - u_{2,0,H}) w_{1,\tilde{h}} \mathrm{d}x, \tag{14}$$

$$B_1(v_{1,\tilde{h}}, \xi_{1,\tilde{h}}) = F_1(\xi_{1,\tilde{h}}) - B_1(u_{1,0,\tilde{h}}, \xi_{1,\tilde{h}}), \tag{15}$$

$$\int_{\mathcal{O}} (v_{2,H} - v_{1,\tilde{h}}) w_{2,H} \mathrm{d}x - B_{2,H}(w_{2,H}, \lambda_{2,H}) = \int_{\mathcal{O}} (u_{1,0,\tilde{h}} - u_{2,0,H}) w_{2,H} \mathrm{d}x, \tag{16}$$

$$B_{2,H}(v_{2,H}, \xi_{2,H}) = F_2(\xi_{2,H}) - B_{2,H}(u_{2,0,H}, \xi_{2,H}), \tag{17}$$

for all $w_{1,\tilde{h}} \in V_D^p(\omega_1, \mathcal{T}_{\tilde{h}})$, $\xi_{1,\tilde{h}} \in V_0^p(\omega_1, \mathcal{T}_{\tilde{h}})$, $w_{2,H} \in V_D^p(\omega_2, \mathcal{T}_H)$, and $\xi_{2,H} \in V_0^p(\omega_2, \mathcal{T}_H)$.
The optimality system (14) to (17) can be written in matrix form as

$$\begin{pmatrix} M & -B^\top \\ B & 0 \end{pmatrix} U = G, \tag{18}$$

where the unknown vector U is given by $U = (v_{1,\tilde{h}}, v_{2,H}, \lambda_{1,\tilde{h}}, \lambda_{2,H})^\top$, and

$$M(\{v_{1,\tilde{h}}, v_{2,H}\}, \{w_{1,\tilde{h}}, w_{2,H}\}) = \begin{pmatrix} \int_{\mathcal{O}} v_{1,\tilde{h}} w_{1,\tilde{h}} \mathrm{d}x & -\int_{\mathcal{O}} v_{2,H} w_{1,\tilde{h}} \mathrm{d}x \\ -\int_{\mathcal{O}} v_{1,\tilde{h}} w_{2,H} \mathrm{d}x & \int_{\mathcal{O}} v_{2,H} w_{2,H} \mathrm{d}x \end{pmatrix},$$

$$B(\{v_{1,\tilde{h}}, v_{2,H}\}, \{\lambda_{1,\tilde{h}}, \lambda_{2,H}\}) = \begin{pmatrix} B_1(v_{1,\tilde{h}}, \lambda_{1,\tilde{h}}) & 0 \\ 0 & B_{2,H}(v_{2,H}, \lambda_{2,H}) \end{pmatrix}.$$

Fully discrete error estimates The coupling solution, denoted by $\bar{u}_{\tilde{h}H}$, is defined as

$$\bar{u}_{\tilde{h}H} = \begin{cases} u_{1,\tilde{h}}(\theta_{1,\tilde{h}}), & \text{in } \omega^+, \\ u^{rec}_{2,H}(\theta_{2,H}), & \text{in } \Omega \setminus \omega^+, \end{cases} \tag{19}$$

where $u^{rec}_{2,H}(\theta_{2,H})$ is a fine scale approximation obtained from the coarse scale solution $u_{2,H}(\theta_{2,H})$ using a post-processing procedure in the following way. We assume that the tensor a_2^ε is Y-periodic in y and we restrict the FE spaces to piecewise FE spaces. Periodic coupling is then used with sampling domains K_ε of size ε. The reconstructed solution $u^{rec}_{2,H}(\theta_{2,H})$ is given by

$$u^{rec}_{2,H}(x) = u_{2,H}(x) + \sum_{j=1}^{d} \psi^{j,h}_{K_\varepsilon}(x) \frac{\partial u_{2,H}}{\partial x_j}(x), \quad x \in K,$$

where $\psi^{j,h}_{K_\varepsilon}$ are the micro solutions of (13) in the sampling domain K_ε. As the numerical solutions might be discontinuous in ω_2, we consider a broken H^1 semi-norm,

$$\|v\|^2_{\bar{\mathrm{H}}^1(\Omega)} := \sum_{K\in\mathcal{T}_h(\omega^+)} \|\nabla v\|^2_{\mathrm{L}^2(K)} + \sum_{K\in\mathcal{T}_H(\Omega\setminus\omega^+)} \|\nabla v\|^2_{\mathrm{L}^2(K)}.$$

We next state our main convergence result for the optimization based numerical solution. Let $u^H \in V_0^1(\omega_2,\mathcal{T}_H)$ be the FE-HMM approximation of the homogenized solution u^0.

Theorem 3.1 (A priori error analysis in ω^+) *Let ε_0 be given by the strong Cauchy-Schwarz Lemma 5.3 and consider $\varepsilon \le \varepsilon_0$. Let u^ε and u^0 be the exact solutions of problems* (1) *and* (10)*, respectively, and $\bar{u}_{\tilde{h}H}$ be the numerical solution of the coupling* (19)*. Further, let $u^H \in V_0^1(\omega_2,\mathcal{T}_H)$ be the FE-HMM approximation of u^0. Assume $u^\varepsilon \in H^{s+1}(\Omega)$, with $s \le 1$, $u^0 \in H^2(\omega_2)$, and assume that* (11) *holds, then*

$$\|u^\varepsilon - u_{1,\tilde{h}}(\theta_{1,\tilde{h}})\|_{\bar{\mathrm{H}}^1(\omega^+)} \le C_1\tilde{h}^s|u^\varepsilon|_{H^{s+1}(\omega_1)} + \frac{C_2}{\tau-\tau^+}\left(\tilde{h}^{s+1}|u^\varepsilon|_{H^{s+1}(\omega_1)} + \varepsilon + e_{HMM,L^2}\right),$$

where the constants are independent of ε, H, $\tilde{h}$, and h, and where $e_{HMM,L^2} = \|u^0 - u^H\|_{\mathrm{L}^2(\omega_2)}$.

Proof. Follows the lines of [7, Theorem 4.3], using a continuous macro FEM (FE-HMM) instead of a discontinuous Galerkin FEM (DG-FE-HMM). □

The Analysis of the error e_{HMM,L^2} is by now standard for the FE-HMM. One decompose the error into [2]

$$e_{HMM,L^2} = \|u^0 - u^H\|_{\mathrm{L}^2(\omega_2)} \le \underbrace{\|u^0 - u^0_H\|_{\mathrm{L}^2(\omega_2)}}_{e_{MAC}} + \underbrace{\|u^0_H - \bar{u}^H\|_{\mathrm{L}^2(\omega_2)}}_{e_{MOD}} + \underbrace{\|\bar{u}^H - u^H\|_{\mathrm{L}^2(\omega_2)}}_{e_{MIC}},$$

where u^0_H is a FEM approximation of u^0 with numerical quadrature and $\bar{u}^H$ is a semi-discrete FE-HMM approximation of u^0, where the micro functions are in the exact Sobolev space $W(K_\delta)$. Under suitable regularity assumption [12], we have

$$e_{MAC} \le CH^2,$$

where the constant C is independent of ε, $\tilde{h}$, H, and h.

Next, following [1, 2] we can bound the micro and modeling errors. If we assume the following regularity on $\psi^i_{K_\varepsilon} \in W(K_\delta)$, the non-discretized micro solutions of problem (13),

$$|\psi^i_{K_\delta}|_{H^2(K_\delta)} \le C\varepsilon^{-1}\sqrt{|K_\delta|}, \quad \text{for } i = 1,\dots,d,$$

we obtain a bound on the micro error

$$e_{MIC} \le C\left(\frac{h}{\varepsilon}\right)^2,$$

where the constant C is independent of ε, $\tilde{h}$, H, and h (we recall that for the reconstruction we use periodic boundary conditions in the micro problems (13) over sampling domains are of size $\delta = \varepsilon$). If we collocate (i.e., freeze) the slow variable x to the quadrature point x_K in the tensor a^ε_2, i.e., we consider $a^\varepsilon_2(x_K, x/\varepsilon)$ in the macro and micro bilinear forms, we obtain an optimal modeling error

$$e_{MOD} = 0, \text{ with } S^1(K_\delta,\mathcal{T}_h) \subset W^1_{per}(K_\delta),$$

assuming that $\delta/\varepsilon \in \mathbb{N}_{>0}$. Without collocation, the modeling error becomes

$$e_{MOD} = C\varepsilon,$$

where the constant C is independent of ε, $\tilde{h}$, H, and h.

Remark 3.2 *When $\delta/\varepsilon \notin \mathbb{N}$ and $\delta > \varepsilon$, Dirichlet boundary conditions are used instead of the periodic conditions in the micro problems* (13)*, and the modeling error becomes*

$$e_{MOD} = \begin{cases} C_1 \frac{\varepsilon}{\delta}, & \text{with collocation and } S^1(K_\delta, \mathcal{T}_h) \subset H_0^1(K_\delta), \\ C_2(\delta + \frac{\varepsilon}{\delta}), & \text{without collocation and } S^1(K_\delta, \mathcal{T}_h) \subset H_0^1(K_\delta), \end{cases}$$

where the constants are independent of ε,δ, $\tilde{h}$, H, and h.

Remark 3.3 *Higher order FE macro and micro spaces can also be considered, and we refer to [2, 3] for details.*

Next, we state an error estimates in the coarse scale region for the optimization based numerical solution with correctors.

Theorem 3.4 (Error estimates in $\Omega \setminus \omega^+$) *Let u^ε be the exact solution of problem* (1) *and $\bar{u}_{\tilde{h}H}$ be the numerical solution of the coupling* (19)*. Let $a_2^\varepsilon(x) = a_2(x, x/\varepsilon)$, where $a_2(x, y)$ is Y-periodic in y and satisfies $a_2(x, y) \in \mathcal{C}(\overline{\omega}_2; L^\infty_{per}(Y))$. Let $\psi^j_{K_\varepsilon}(x) \in W^1_{per}(K_\varepsilon)$, $j = 1, \ldots, d$. If in addition, $u^\varepsilon \in H^2(\Omega)$, $u_2^0(\theta_2) \in H^2(\omega_2)$, $u_1^\varepsilon \in H^{s+1}(\omega_1)$, with $s \leq 1$, and $\psi^j_{K_\varepsilon}(x) \in W^{1,\infty}(K_\varepsilon)$, $j = 1, \ldots, d$. It holds,*

$$\begin{aligned} \|u_2^{rec}(\theta_2) - u_{2,H}^{rec}(\theta_2^H)\|_{\bar{\mathrm{H}}^1(\Omega\setminus\omega^+)} \leq\ & C_1\varepsilon^{1/2} + C_2\left(\frac{h}{\varepsilon}\right) + C_3 H|u_2^0|_{H^2(\omega_2)} \\ & + \frac{C_4}{\tau^+}\left(\tilde{h}^{s+1}|u_1^\varepsilon|_{H^{s+1}(\omega_1)} + \varepsilon + H^2|u_2^0|_{H^2(\omega_2)}\right). \end{aligned}$$

where the constants are independent of $H, \tilde{h}, h$, and ε.

Proof. Follows the lines of [7, Theorem 4.4], where DG-FE-HMM is replaced by FE-HMM. □

Remark 3.5 *We note that the above theorem is also valid when using discontinuous Galerkin macro solver (i.e., the DG-FE-HMM [4]). This has been studied in [7] for the cost function of case 1. A similar proof applies for the cost function of case 2.*

4 Numerical experiments

In this section, we give three numerical experiments that can be seen as a complement of the ones carried in [7], where we focused on a minimization in $L^2(\omega_0)$, with interior subdomains and matching grids in the overlap ω_0. In the first experiment, we still consider the minimization over $L^2(\omega_0)$ and compare matching and non-matching meshes. The second experiment illustrates the coupling with the cost function of case 2 over $\Gamma_1 \cup \Gamma_2$, and comparisons with the cost function of case 1 over ω_0. In the last example, we combine non-matching grids and a minimization over the boundary. We observe several order of magnitude of saving in computational cost when compared to the method proposed in [7].

Comparison of matching and non-matching grids on the overlap.

Experiment 1. For this experiment, we use the cost function of case 1

$$J(\mu_1,\mu_2)=\frac{1}{2}\|u_1^\varepsilon(\mu_1)-u_2^0(\mu_2)\|^2_{\mathrm{L}^2(\omega_0)}.$$

Using FEM and FE-HMM in ω_1 and ω_2 respectively, leads to two main restrictions: the mesh size in ω_1 should be smaller than the fine scale, whereas the mesh size in ω_2 can be larger than the fine scales, in order to take full advantage of the FE-HMM. Since both methods are defined in ω_0, we can chose to have the same FE in both meshes on the overlap, or one can impose two different meshes. With the first choice, no interpolations must be considered between $\mathcal{T}_{\tilde{h}}$ and $\mathcal{T}_H$ over ω_0, but $\mathcal{T}_H$ is composed of FE with mesh size as small as the fine scales. In that situation, DG-FE-HMM is chosen instead of FE-HMM due to the discontinuity at the interface Γ_1. The second choice requires interpolation between the meshes in ω_0, but $\mathcal{T}_H$ is not restricted by the size of the fine mesh $\mathcal{T}_{\tilde{h}}$. We show that both cases give similar convergence rates, but the computational cost is significantly reduced in the second case.
Let us consider a Dirichlet elliptic boundary value in $\Omega=[0,1]^2$,

$$\begin{aligned}-\mathrm{div}\,(a^\varepsilon\nabla u^\varepsilon) &= f,\ \text{in } \Omega,\\ u &= 0,\ \text{on } \partial\Omega,\end{aligned}$$

with $f\equiv 1$ and a^ε is given by

$$a_2^\varepsilon(x_1,x_2)=\frac{1}{6}\Big(\frac{1.1+\sin(2\pi(x_1/\varepsilon)(x_2/\varepsilon))}{1.1+\sin(2\pi x_2/\varepsilon)}+\sin(4x_1^2x_2^2)+2\Big)I_2,$$

$$a_\omega(x_1,x_2)=3+\frac{1}{7}\sum_{j=0}^{4}\sum_{i=0}^{j}\frac{2}{j+1}\cos\left(\lfloor 8\left(ix_2-x_1/(i+1)\right)\rfloor+\lfloor 150ix_1\rfloor+\lfloor 150x_2\rfloor\right).$$

Let x_c be the center of Ω, we consider $\omega_1=x_c+[-1/4,1/4]I_2$ and $\omega=x_c+[-1/8,1/8]I_2$. Let $H=1/8$, $\varepsilon=1/10$, and a micro mesh size $h=\varepsilon/L$, so that the micro error is negligible. We initialize the fine mesh to $\tilde{h}=1/16$. We use uniform simplicial meshes in ω_1 and ω_2, and assume that $\mathcal{T}_{\tilde{h}}$ is obtained from $\mathcal{T}_H$ using a uniform refinement in ω_0. This allows simplification in the interpolation between the two meshes in the overlap. We couple the FEM over ω_1 with the mesh $\mathcal{T}_{\tilde{h}}(\omega_1)$ with the FE-HMM over ω_2 with mesh $\mathcal{T}_H(\omega_2)$, and compare it with a coupling between FEM over $\mathcal{T}_{\tilde{h}}(\omega_1)$ with DG-FE-HMM over a mesh composed of coarse FE from $\mathcal{T}_H(\omega_2\setminus\omega_0)$ with small FE from the fine mesh $\mathcal{T}_{\tilde{h}}(\omega_0)$. The reference fine scale solution is computed on a very fine mesh, and we compare the two numerical solutions with the reference one. After three i terations, we plot the numerical approximations of the fine scale solution u_1^ε and coarse scale solution u_2^0 (in transparent), for a coupling with minimization of the cost function of case 1 with non-matching grid (Figure 2(a)) and with matching grids (Figure 2(b)). A zoom of the coarse scale solutions in the overlap region ω_0 can be seen in Figure 2(c) for the coupling with non-matching grids and in Figure 2(d) with matching grids, where the coupling is performed with the cost function of case 1 (as the fine meshes become too dense after three iterations, we plot for the zoom the solution after one iteration to better visualize the difference in the meshes).
We refine either only in ω_1 for the fine scale solver (non-matching grids) or in addition in ω_0 for the coarse scale solver (matching grids). We set $\delta=\varepsilon$ for the sampling domains, and consider a micro mesh size $h=\varepsilon/L$, so that the micro error is negligible. Figure 3(a) shows the H^1 norm in ω with

non-matching grids (bullet) and with matching grids (diamond); we see that the errors are similar. We also measured the times, using Matlab timer, to compute the numerical solutions. We see in Figure 3(b) that using non-matching grids is faster as the number of micro problems, that have to be computed with the coarse solver, is smaller and fixed, whereas it increases when matching grids are used, causing a significant time overhead.

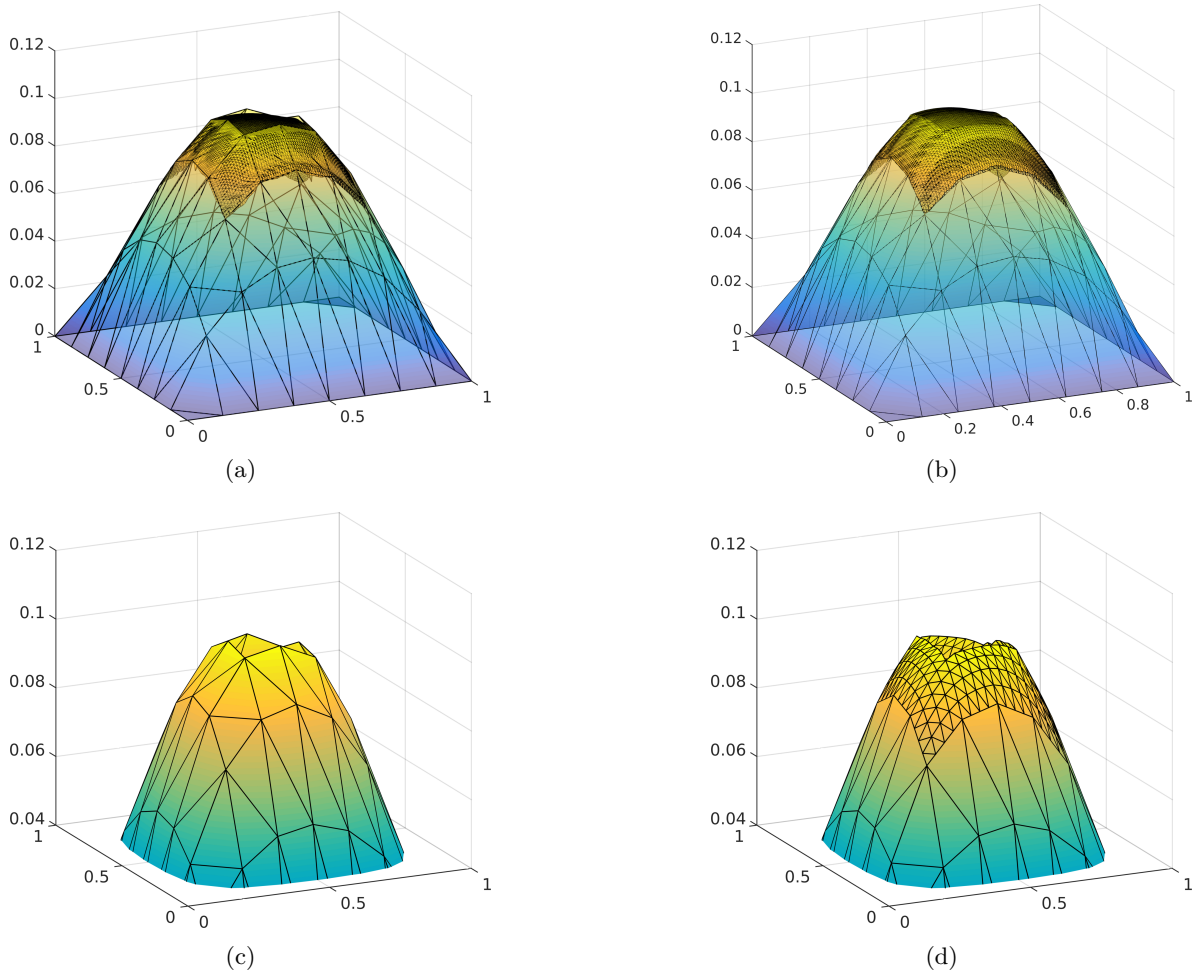

Figure 2: experiment 1: numerical solutions of the coupling with minimization of the cost function of case 1 using non-matching grids (a) and matching grids (b), zoom in ω_0 of the coarse scale solution with the cost function of case 1 and non-matching grids (c) and with matching grids (d).

The rate of convergence in ω is influenced by H and ε, and when $\tilde{h}$ is refined, we expect a saturation, depending on H and ε, in the convergence. Let $\varepsilon = 1/20$ and initialize the fine mesh to $\tilde{h} = 1/64$. We set $H = 1/8, 1/16$, and $1/32$, and refine $\tilde{h}$ in each iteration. In Figure 4, we plot the H^1 norm between the reference and numerical solutions w.r.t the mesh size in ω. We see indeed that the error saturates at a threshold value that depends on H.

Minimization with interface control.

For this experiment, we compare the coupling done with the cost function of case 1 and of case 2 on

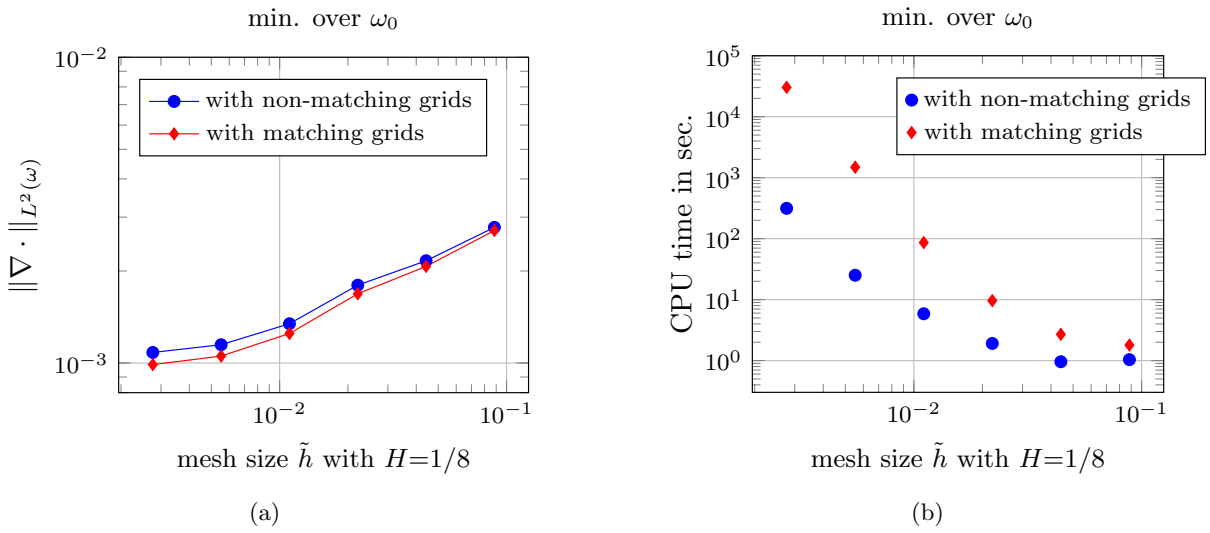

Figure 3: experiment 1: (a) H^1 norm in ω with minimization of the cost function of case 1 using non-matching grids (bullet) and matching grids (diamond), (b) CPU time with the cost function of case 1 using non-matching grids (bullet) and matching grids (diamond).

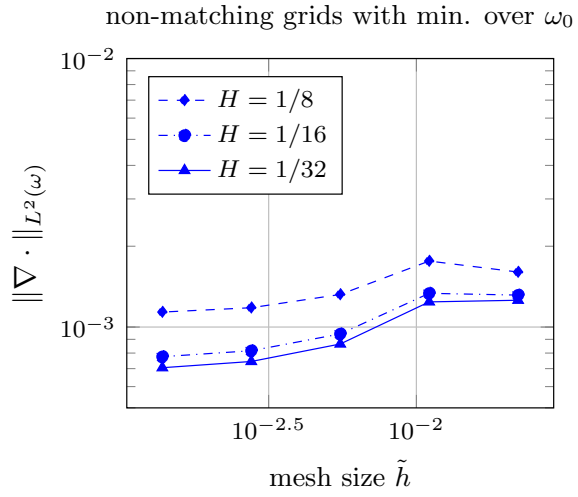

Figure 4: experiment 1:(a) H^1 norm between the reference and numerical solution using non-matching grids and cost function of case 1 for different macro mesh size $H = 1/8$ (dashes), $H = 1/16$ (dash-dots), and $H = 1/32$ (full).

an elliptic problem with $\omega \subseteq \Omega$, i.e., when the boundaries of ω and Ω intersect (see Figure 1 right picture).

Experiment 2. Let us consider a Dirichlet elliptic boundary value in $\Omega = [0,1]^2$,

$$\begin{aligned} -\mathrm{div}\,(a^\varepsilon \nabla u^\varepsilon) &= f, \text{ in } \Omega, \\ u &= 0, \text{ on } \partial\Omega, \end{aligned}$$

with $f \equiv 1$ and a^ε – plotted in Figure 5(b) – is given by

$$\begin{aligned} a_2^\varepsilon(x_1,x_2) &= (\cos(2\pi x_1/\varepsilon)+2)I_2, \\ a_\omega(x_1,x_2) &= 3 + \frac{1}{7}\sum_{j=0}^{4}\sum_{i=0}^{j}\frac{2}{j+1}\cos\left(\lfloor 8\left(ix_2 - x_1/(i+1)\right)\rfloor + \lfloor 150 i x_1\rfloor + \lfloor 150 x_2\rfloor\right). \end{aligned}$$

The tensor a^ε in ω_2 has scale separation, is Y-periodic in the fast variable, and the homogeneous tensor a_2^0 can be explicitly derived as

$$a_2^0(x) = \begin{pmatrix} \left(\int_0^1 \frac{1}{a(y_1)}\mathrm{d}y_1\right)^{-1} & 0 \\ 0 & 2 \end{pmatrix}.$$

Let $\omega_1 = [0,1/2]\times y$ and $\omega = [0,1/4]\times y$, with $y \in [0,1]$. An illustration of a numerical solution is given in Figure 6(a). At first, we consider the cost of case 1,

$$J(\mu_1,\mu_2) = \frac{1}{2}\|u_1^\varepsilon(\mu_1) - u_2^0(\mu_2)\|^2_{\mathrm{L}^2(\omega_0)}.$$

Let $\varepsilon = 1/50$, and $h/\varepsilon = 1/L$ be small enough to neglect the micro error. We initialize the fine mesh to $\tilde{h} = 1/128$. For different macro mesh sizes $H = 1/8, 1/16, 1/32$ and $1/64$, we refine $\tilde{h}$ and monitor the convergence rates between the numerical solution of the coupling and the reference solution. In Figure 5(a), the H^1 norm is displayed for $H = 1/8$ (dots), $H = 1/16$ (dashes-dots), $H = 1/32$ (dashes) and $H = 1/64$ (full lines). One can see that the error saturate at a value depending on the macro mesh size H.

Now, we compare the costs of case 1 over ω_0 with the cost of case 2 over $\Gamma_1 \cup \Gamma_2$. We fix $\varepsilon = 1/10$, $H = 1/16$, and $h = \varepsilon/L$ small enough in order to neglect the micro error. We initialize the fine mesh to $\tilde{h} = 1/32$ and refine the mesh only in ω_1. The numerical approximations of u_1^ε and u_2^0 are shown in Figure 6(a), for the cost of case 1 over ω_0, and in Figure 6(b), for the cost of case 2 over $\Gamma_1 \cup \Gamma_2$. The H^1 and L^2 errors between u^H and a reference solution in ω_0, are shown in Figures 6(c) and 6(d), respectively. Computational times are compared as well in Figure 7, for the cost over ω_0 (diamonds) and the cost over $\Gamma_1 \cup \Gamma_2$ (bullets). As the number of degrees of freedom of the saddle point problem (18) is reduced when minimizing over the boundaries $\Gamma_1 \cup \Gamma_2$, we see that the coupling over ω_0 is more costly than the coupling over $\Gamma_1 \cup \Gamma_2$. Considering an interpolation between the two meshes in the interface ω_0 gives similar results as, due to the periodicity of a_2^ε, we need only to resolve one cell problem to compute the homogenized tensor a_2^0.
We next vary the size of the overlap ω_0, and consider $\omega_1 = [0, 1/4 + mH]\times y$, for $m = 1, 4, 8$, where $H = 1/32$ is the coarse mesh size, and initialize $\tilde{h} = 1/64$. We minimize over the overlap ω_0. We observe that both couplings are influenced by the size of $\tau = \mathrm{dist}(\Gamma_1 \cup \Gamma_2)$ and this is shown in the H^1 errors in Figure 8. The rates deteriorate when τ goes to zero.

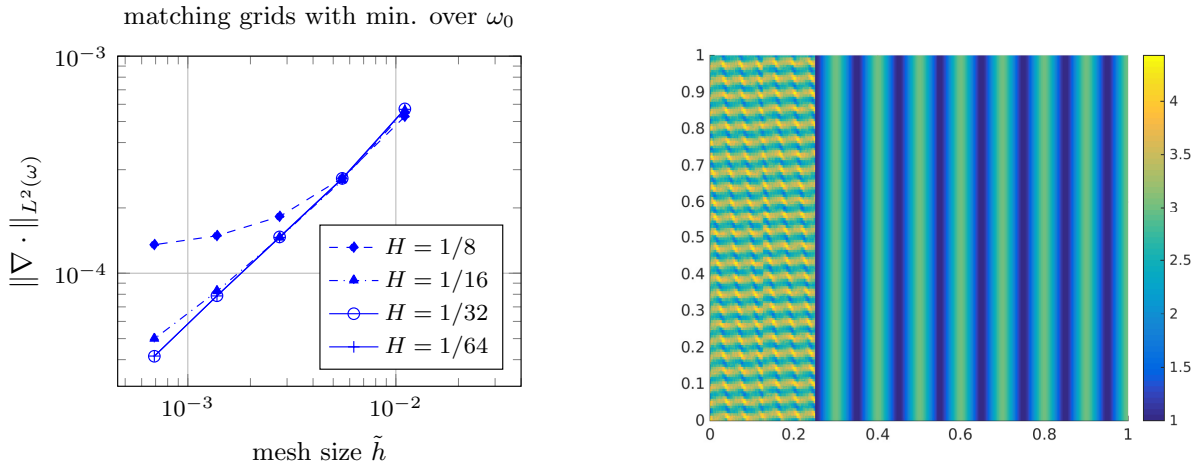

Figure 5: experiment 2: (a) H^1 errors between the numerical and the reference solutions in ω using matching grids and the cost function of case 1 with different macro mesh size $H = 1/8$ (stars), $H = 1/16$ (diamonds), $H = 1/32$ (bullets), and $H = 1/64$ (plus), (b) tensor a^ε over Ω for $\varepsilon = 1/10$.

Minimization with interface control on non-matching grids.

For the last experiment, we combine the two previous effects. The fastest coupling is obtained by performing by considering the minimization with of the cost of case 2 with interpolation of the two meshes in the overlap, whereas the slowest coupling is obtained by the minimization with the cost function of case 1 using identical meshes in the overlap.

Experiment 3. We consider a Dirichlet elliptic boundary value in $\Omega = [0,1]^2$,

$$\begin{aligned} -\mathrm{div}\,(a^\varepsilon \nabla u^\varepsilon) &= f, \text{ in } \Omega, \\ u &= 0, \text{ on } \partial\Omega, \end{aligned}$$

with $f \equiv 1$ and a^ε is given by

$$a_2^\varepsilon(x_1,x_2) = \frac{1}{6}\left(\frac{1.1+\sin(2\pi(x_1/\varepsilon)(x_2/\varepsilon))}{1.1+\sin(2\pi x_2/\varepsilon)} + \sin(4x_1^2x_2^2) + 2\right) I_2,$$

$$a_\omega(x_1,x_2) = 3 + \frac{1}{7}\sum_{j=0}^{4}\sum_{i=0}^{j}\frac{2}{j+1}\cos\left(\lfloor 8\left(ix_2 - x_1/(i+1)\right)\rfloor + \lfloor 150 i x_1\rfloor + \lfloor 150 x_2\rfloor\right).$$

We set $H = 1/16$ and $\varepsilon = 1/10$. We initialize $\tilde{h} = 1/32$. In Figure 9(a), we see the H^1 error for the two settings are similar whereas the computational cost using minimization over the overlap and non-matching grid in ω_0 dramatically decrease (see Figure 9(b)).

5 Appendix

Let us start by recalling the Caccioppoli inequality [19]. Let $\omega \subset \omega_1$ be subdomains of Ω with $\tau = \mathrm{dist}(\partial\omega, \partial\omega_1)$ and set $\Gamma = \partial\Omega$. For a tensor a, the set of a-harmonic functions is denoted by

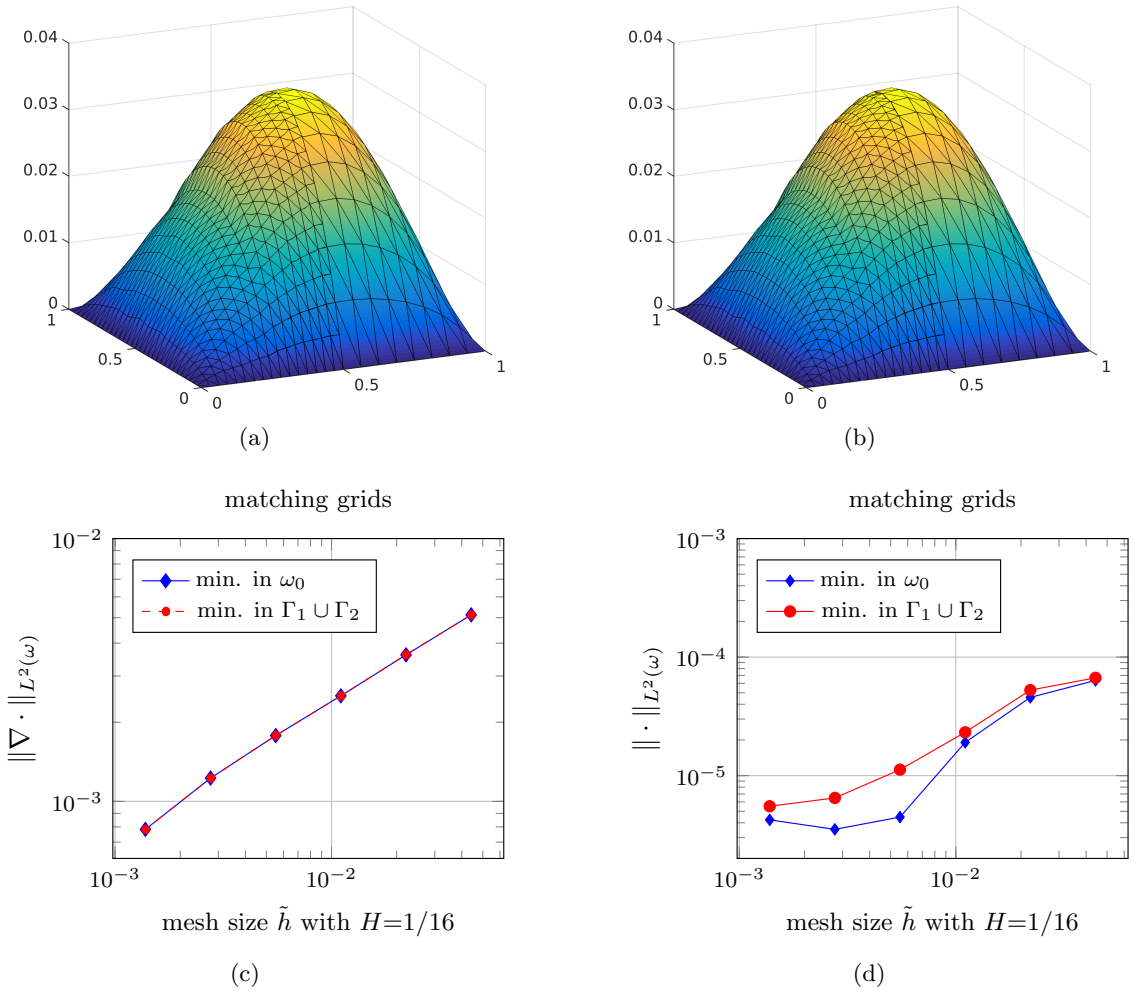

Figure 6: experiment 2: numerical solutions using matching grids and the cost function of case 1 (a) and of case 2 (b), (c) H^1 error between the numerical and reference solutions in ω using matching grids and the cost function of case 1 (diamond) and the cost function of case 2 (bullet), (d) L^2 error between the numerical and reference solutions in ω, using matching grids and the cost function of case 1 (diamond) and the cost function of case 2 (bullet).

$\mathcal{H}(\omega_1)$, and consists of functions $u \in L^2(\omega_1) \cap H^1_{\text{loc}}(\omega_1)$ such that

$$\int_{\omega_1} a\nabla u \cdot \nabla v \mathrm{d}x = 0, \quad \forall v \in \mathcal{C}_0^\infty(\omega_1),$$

where $H^1_{\text{loc}}(\omega_1) := \{u \in H^1(O) \mid \text{ for any open set } O \text{ with } \overline{O} \subset \omega_1\}$.

Theorem 5.1 (Caccioppoli inequality [19]) *Let $u \in \mathcal{H}(\omega_1)$, then*

$$\|\nabla u\|_{\mathrm{L}^2(\omega)} \leq \frac{2\beta^{1/2}}{\alpha^{1/2}\tau}\|u\|_{\mathrm{L}^2(\omega_1)}.$$

Further, it holds,

$$\|\nabla u\|_{\mathrm{L}^2(\omega)} \leq \frac{2\beta^{1/2}}{\alpha^{1/2}\tau}\|u\|_{\mathrm{L}^2(\omega_0)}.$$

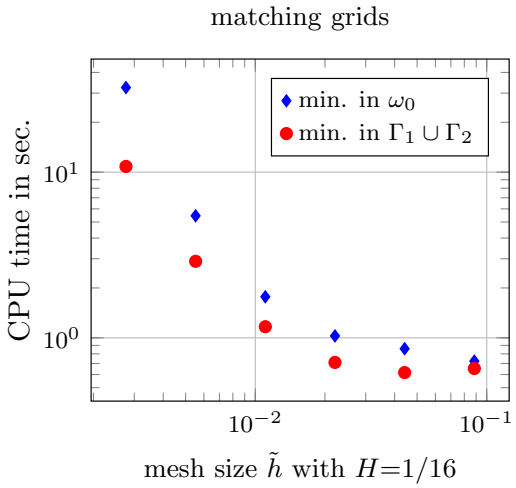

Figure 7: experiment 2: CPU time using matching grids with the cost function of case 1 (diamond) and the cost function of case 2 (bullet).

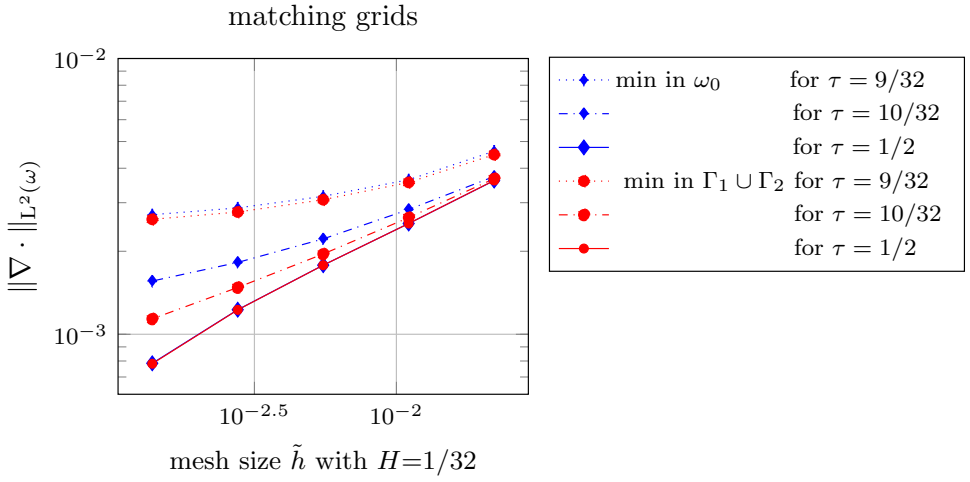

Figure 8: experiment 2: H^1 errors between the numerical and reference solutions in ω with matching grids and the cost function of case 1 (diamond) and the cost function of case 2 (bullet) for $\tau = 9/32$ (dots), $\tau = 10/32$ (dash-dots), and $\tau = 1/2$ (full).

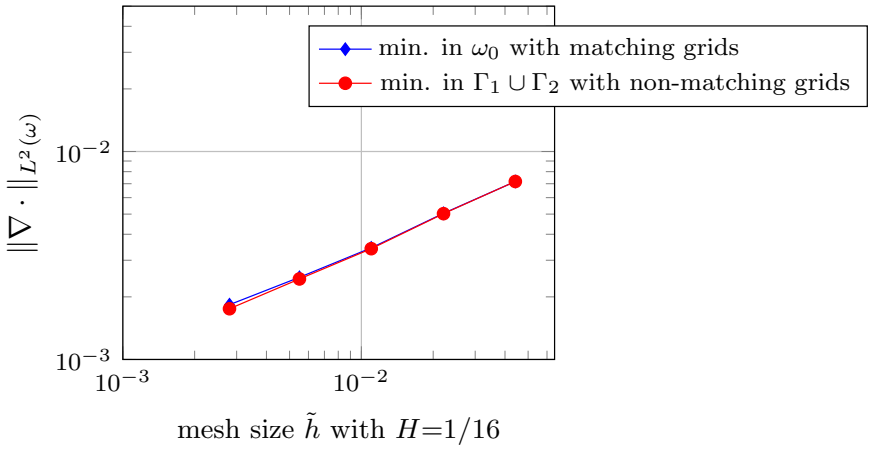

(a)

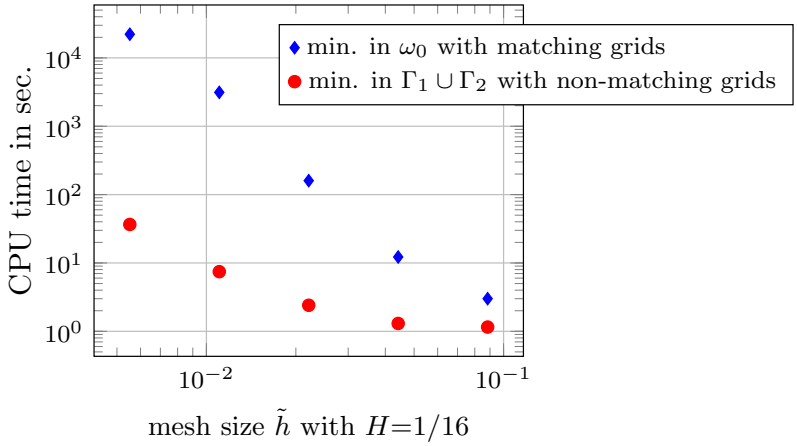

(b)

Figure 9: experiment 3: (a) errors between the numerical and reference solutions with the cost function of case 1 and matching grids (diamond) and with the cost function of case 2 with non-matching grids (bullet), (b) CPU time with the cost function of case 1 and matching grids (diamond) and with the cost function of case 2 with non-matching grids (bullet).

We note that elliptic problems with a non null right hand side, and problems where $\partial\omega \cap \Gamma \neq \emptyset$, can also be considered and we refer to [19] for details. We give next a bound of the L^2 norm over ω by the L^2 norm over the overlap ω_0.

Lemma 5.2 *Let v_1^ε and v_2^0 be solutions of (4), for $i = 1, 2$, respectively. The following bounds hold*

$$\|v_1^\varepsilon\|_{\mathrm{L}^2(\omega)} \leq \frac{C}{\tau}\|v_1^\varepsilon\|_{\mathrm{L}^2(\omega_0)},$$
$$\|v_2^0\|_{\mathrm{L}^2(\Omega\setminus\omega_1)} \leq \frac{C}{\tau}\|v_2^0\|_{\mathrm{L}^2(\omega_0)},$$

where τ is the width of the overlap and C is a constant depending on α, β, and the Poincaré constant associated to ω_1 and ω_2, respectively.

Proof. see [7, Lemma 2.1]. □

In the next lemma, we state a strong version of the Cauchy-Schwarz inequality, and refer to [7] for the proof. Let us recall the problems for the state variables: find $v_i \in H_D^1(\omega_i)$ solution of

$$\begin{aligned} -\mathrm{div}\,(a_i \nabla v_i) &= 0, \quad \text{in } \omega_i, \\ v_i &= \theta_i, \quad \text{on } \Gamma_i, \\ v_i &= 0, \quad \text{on } \partial\omega_i \cup \Gamma_D, \\ n_i \cdot (a_i \nabla v_i) &= 0, \quad \text{on } \partial\omega_i \cap \Gamma_N, \end{aligned} \tag{20}$$

where $a_1 = a_1^\varepsilon$ and $a_2 = a_2^0$.

Lemma 5.3 (Strong Cauchy-Schwarz) *Let $v_1^\varepsilon \in H_D^1(\omega_1)$ and $v_2^0 \in H_D^1(\omega_2)$ be solutions of (20) for $i = 1, 2$. Then, there exist an $\varepsilon_0 > 0$ and a positive constant $C_s < 1$ such that for all $\varepsilon \leq \varepsilon_0$, it holds*

$$\int_{\omega_0} v_1^\varepsilon v_2^0 dx \leq C_s \|v_1^\varepsilon\|_{\mathrm{L}^2(\omega_0)} \|v_2^0\|_{\mathrm{L}^2(\omega_0)}.$$

Discrete versions of the Caccioppoli and the strong Cauchy-Schwarz inequalities are stated below. $v^h \in V^p(\omega_1, \mathcal{T}_h)$ solution of

$$B_1(v^h, w^h) := \int_{\omega_1} a \nabla v^h \cdot \nabla w^h \mathrm{d}x = 0, \quad \forall w^h \in V_0^p(\omega_1, \mathcal{T}_h). \tag{21}$$

Lemma 5.4 (Discrete Caccioppoli inequality for interior domains, [26]) *Let $v^h \in V^p(\omega_1, \mathcal{T}_h)$ satisfy equation (21) for all $w^h \in V_0^p(\omega_1, \mathcal{T}_h)$; it holds*

$$\|\nabla v^h\|_{\mathrm{L}^2(\omega)} \leq C\frac{1}{\tau}\|v^h\|_{\mathrm{L}^2(\omega_1)},$$

where the constant C is independent of h.

We now give the discrete strong Cauchy-Schwarz inequality, and to simplify the notations, we omit the ε dependency in v_1.

Lemma 5.5 *Let $\varepsilon < \varepsilon_0$ and $C_s < 1$ be given by the strong Cauchy-Schwarz Lemma 5.3, and let $v_{1,\tilde{h}} \in V_D^p(\omega_1, \mathcal{T}_{\tilde{h}})$ and $v_{2,H} \in V_D^p(\omega_2, \mathcal{T}_H)$ be numerical solutions of (18). There exist $\tilde{h}_0 > 0$ and $H_0 > 0$ such that*

$$\int_{\omega_0} v_{1,\tilde{h}} v_{2,H} dx \leq C_s \|v_{1,\tilde{h}}\|_{\mathrm{L}^2(\omega_0)} \|v_{2,H}\|_{\mathrm{L}^2(\omega_0)}, \quad \forall \tilde{h} < \tilde{h}_0, H < H_0.$$

References

[1] Abdulle, A. On a priori error analysis of fully discrete heterogeneous multiscale FEM. *Multiscale Model. Simul. 4*, 2 (2005), 447–459.

[2] Abdulle, A. The finite element heterogeneous multiscale method: a computational strategy for multiscale PDEs. In *Multiple scales problems in biomathematics, mechanics, physics and numerics*, vol. 31 of *GAKUTO Internat. Ser. Math. Sci. Appl.* Gakkōtosho, Tokyo, 2009, pp. 133–181.

[3] Abdulle, A. A priori and a posteriori error analysis for numerical homogenization: a unified framework. *Ser. Contemp. Appl. Math. CAM 16* (2011), 280–305.

[4] Abdulle, A. Discontinuous Galerkin finite element heterogeneous multiscale method for elliptic problems with multiple scales. *Math. Comp. 81*, 278 (2012), 687–713.

[5] Abdulle, A., E, W., Engquist, B., and Vanden-Eijnden, E. The heterogeneous multiscale method. *Acta Numer. 21* (2012), 1–87.

[6] Abdulle, A., and Jecker, O. An optimization-based, heterogeneous to homogeneous coupling method. *Commun. Math. Sci. 13*, 6 (2015), 1639–1648.

[7] Abdulle, A., Jecker, O., and Shapeev, A. V. An optimization based coupling method for multiscale problems. to appear in Multiscale Model. Simul., SIAM.

[8] Babuška, I., and Lipton, R. L2-global to local projection an approach to multiscale analysis. *Math. Models and Meth. in Appl. Science 21* (2011), 2211–2226.

[9] Bensoussan, A., Lions, J.-L., and Papanicolaou, G. *Asymptotic analysis for periodic structures*. North-Holland Publishing Co., Amsterdam, 1978.

[10] Blanc, X., Le Bris, C., and Lions, P.-L. A possible homogenization approach for the numerical simulation of periodic microstructures with defects. *Milan J. Math. 80* (2012), 351–367.

[11] Ciarlet, P. G. *The finite element method for elliptic problems*, vol. 4 of *Studies in Mathematics and its Applications*. North-Holland, 1978.

[12] Ciarlet, P. G., and Raviart, P. A. Maximum principle and uniform convergence for the finite element method. *Comput. Methods Appl. Mech. Engrg. 2* (1973), 17–31.

[13] D'Elia, M., Perego, M., Bochev, P., and Littlewood, D. A coupling strategy for nonlocal and local diffusion models with mixed volume constraints and boundary conditions. *Computer and Mathematics with Applications 71*, 11 (2016), 2218–2230.

[14] Discacciati, M., Gervasio, P., and Quarteroni, A. The interface control domain decomposition (icdd) method for elliptic problems. *SIAM J. Control Optim. 51*, 5 (2013), 3434–3458.

[15] Efendiev, Y., and Hou, T. Y. *Multiscale finite element methods. Theory and applications*, vol. 4 of *Surveys and Tutorials in the Applied Mathematical Sciences*. Springer, New York, 2009.

[16] Geers, M. G. D., Kouznetsova, V. G., and Brekelmans, W. A. M. Multi-scale computational homogenization: Trends and challenges. *J. Comput. Appl. Math. 234* (2010), 2175–2182.

[17] Gerritsen, M. G., and Durlofsky, L. J. Modeling fluid flow in oil reservoirs. *Annu. Rev. Fluid Mech. 37* (2005), 211–238.

[18] Gervasio, P., Lions, J.-L., and Quarteroni, A. Heterogeneous coupling by virtual control methods. *Numer. Math. 90* (2000), 241–264.

[19] Giaquinta, M. *Multiple integrals in the calculus of variations and nonlinear elliptic systems*. Princeton University Press, 1983.

[20] Henning, P., and Peterseim, D. Oversampling for the Multiscale Finite Element Method. *SIAM Multiscale Model. Simul. 11*, 4 (2013), 1149–1175.

[21] Jikov, V. V., Kozlov, S. M., and Oleinik, O. A. *Homogenization of differential operators and integral functionals*. Springer-Verlag, Berlin, Heidelberg, 1994.

[22] Lions, J.-L. *Optimal Control of systems governed by partial differential equations*. Springer-Verlag, New York, 1971.

[23] Målqvist, A., and Peterseim, D. Localization of elliptic multiscale problems. *Math. Comp. 83*, 290 (2014), 2583–2603.

[24] Moskow, S., and Vogelius, M. First-order corrections to the homogenised eigenvalues of a periodic composite medium. a convergence proof. *Proc. Roy. Soc. Edinburgh 127A* (1997), 1263–1299.

[25] Murat, F., and Tartar, L. H-convergence. In *Topics in the mathematical modelling of composite materials*, vol. 31 of *Progr. Nonlinear Differential Equations Appl.* Birkhäuser Boston, Boston, MA, 1997, pp. 21–43.

[26] Nitsche, J. A., and Schatz, A. H. Interior estimates for ritz-galerkin methods. *Math. Comp. 28*, 128 (1974), 937–958.

[27] Oden, J. T., and Vemaganti, K. S. Estimation of local modeling error and goal-oriented adaptive modeling of heterogeneous materials. I. Error estimates and adaptive algorithms. *J. Comput. Phys. 164*, 1 (2000), 22–47.

[28] Olson, D., Bochev, P. B., Luskin, M., and Shapeev, A. V. An optimization-based atomistic-to-continuum coupling method. *SIAM J. Numer. Anal. 52*, 4 (2014), 2183–2204.